frontiers | Frontiers in Nutrition

TYPE Original Research
PUBLISHED 06 October 2022
DOI 10.3389/fnut.2022.953056

OPEN ACCESS

EDITED BY
Francesco Galli,
University of Perugia, Italy

REVIEWED BY
Desirée Bartolini,
University of Perugia, Italy
Jose Vina,
University of Valencia, Spain

*CORRESPONDENCE
Martha S. Field
mas246@cornell.edu

SPECIALTY SECTION
This article was submitted to Nutrition and Metabolism, a section of the journal Frontiers in Nutrition

RECEIVED 25 May 2022
ACCEPTED 20 September 2022
PUBLISHED 06 October 2022

CITATION
Ortiz SR, Heinz A, Hiller K and Field MS (2022) Erythritol synthesis is elevated in response to oxidative stress and regulated by the non-oxidative pentose phosphate pathway in A549 cells.
Front. Nutr. 9:953056.
doi: 10.3389/fnut.2022.953056

Erythritol synthesis is elevated in response to oxidative stress and regulated by the non-oxidative pentose phosphate pathway in A549 cells

Semira R. Ortiz[1], Alexander Heinz[2], Karsten Hiller[2] and Martha S. Field[1]*

[1]Division of Nutritional Sciences, Cornell University, Ithaca, NY, United States, [2]Department of Bioinformatics and Biochemistry, Braunschweig Integrated Centre of Systems Biology (BRICS), Technische Universität Braunschweig, Braunschweig, Germany

Background: Erythritol is a predictive biomarker of cardiometabolic diseases and is produced from glucose metabolism through the pentose phosphate pathway (PPP). Little is known regarding the regulation of endogenous erythritol synthesis in humans.

Objective: In the present study, we investigated the stimuli that promote erythritol synthesis in human lung carcinoma cells and characterized potential points of regulation along the PPP.

Methods: Human A549 lung carcinoma cells were chosen for their known ability to synthesize erythritol. A549 cells were treated with potential substrates for erythritol production, including glucose, fructose, and glycerol. Using siRNA knockdown, we assessed the necessity of enzymes G6PD, TKT, TALDO, and SORD for erythritol synthesis. We also used position-specific ^{13}C-glucose tracers to determine whether the carbons for erythritol synthesis are derived directly from glycolysis or through the oxidative PPP. Finally, we assessed if erythritol synthesis responds to oxidative stress using chemical and genetic models.

Results: Intracellular erythritol was directly associated with media glucose concentration. In addition, siRNA knockdown of TKT or SORD inhibited erythritol synthesis, whereas siG6PD did not. Both chemically induced oxidative stress and constitutive activation of the antioxidant response transcription factor NRF2 elevated intracellular erythritol.

Conclusion: Our findings indicate that in A549 cells, erythritol synthesis is proportional to flux through the PPP and is regulated by non-oxidative PPP enzymes.

KEYWORDS

erythritol, oxidative stress, pentose phosphate pathway, glucose metabolism, cardiometabolic diseases

Introduction

Serum erythritol is a predictive biomarker of chronic disease onset and associated complications. In one large prospective cohort, baseline serum erythritol was elevated in subjects who developed cardiovascular disease (CVD) or type 2 diabetes mellitus (T2DM) up to 20 years later (1, 2). Another recent study compared patients with cardiovascular risk factors who did and did not develop coronary artery disease. Serum erythritol was significantly elevated in those who did develop coronary artery disease. Erythritol has also been shown to predict risk for diabetic complications including retinopathy, nephropathy, and arterial stiffness (3–5). Serum erythritol appears to be an early, general marker of cardiometabolic dysfunction.

Erythritol is a four-carbon polyol that was recently found to be endogenously synthesized in humans. Little is known regarding the regulation of erythritol synthesis. Hootman et al. first demonstrated that erythritol is produced from glucose in humans through the pentose phosphate pathway (PPP) (6). It was further identified that the enzymes sorbitol dehydrogenase (SORD) and alcohol dehydrogenase 1 (ADH1) are responsible for catalyzing the final step in erythritol synthesis from glucose (namely conversion of erythrose to erythritol) using the cofactor NADPH (7). These findings were validated in human lung carcinoma A549 cells (7).

The PPP branches off from glycolysis and fuels anabolic reactions. It consists of two phases: the oxidative PPP and the non-oxidative PPP. The oxidative PPP generates NADPH, which is essential for endogenous antioxidant generation and lipid synthesis. The non-oxidative PPP consists of a series of sugar interconversions that provide precursors for nucleotide synthesis. The non-oxidative phase can convert pentoses back to glycolytic intermediates through reversible reactions. PPP metabolism plays roles in the development of cardiometabolic diseases across multiple organs. The rate limiting enzyme of the PPP, glucose-6-phosphate dehydrogenase (G6PD), is elevated in the adipose tissue and skeletal muscle of prediabetic subjects (8, 9). In adipose tissue, elevated G6PD promotes pro-inflammatory macrophages, exacerbating insulin resistance (9). In skeletal muscle cells, inhibition of G6PD can improve insulin-stimulated glucose uptake (8). PPP flux is also important in the liver, where NADPH synthesis can contribute to fatty liver development (10).

As a product of the PPP, erythritol synthesis may be an indicator of high PPP flux and the associated aberrant changes in glucose metabolism. A549 cells are a useful model to evaluate intracellular erythritol dynamics due to their high rate of PPP activity (11, 12). The purpose of this study was to identify the upstream factors that regulate erythritol synthesis. Our findings highlight that, in cancer cells, erythritol synthesis is increased in response to PPP stressors and is primarily regulated by glucose availability and activity of enzymes within the non-oxidative PPP.

Abbreviations: ADH1, alcohol dehydrogenase 1; Alpha MEM, Minimum Essential Medium Alpha Modification; ATUB, alpha tubulin; DMEM, Dulbecco's Modified Eagle Medium; ECAR, extracellular acidification rate; GAPDH, glyceraldehyde-3-phosphate dehydrogenase; G6PD, glucose-6-phosphate dehydrogenase; GSSG, oxidized glutathione; KEAP1, kelch like ECH associated protein 1; NRF2, nuclear factor-erythroid factor 2-related factor 2; OCR, oxygen consumption rate; PPP, pentose phosphate pathway; SORD, sorbitol dehydrogenase; TALDO, transaldolase; TKT, transketolase; WT, wildtype.

Materials and methods

Cell culture and treatment with carbohydrates

A549 cells were obtained from ATCC (CCL-185) and maintained in Minimum Essential Medium Alpha Modification (MEM Alpha) containing ribonucleosides, deoxyribonucleosides, phenol red, and l-glutamine, 1% penicillin/streptomycin (Cytiva, Marlborough, MA, USA), and 10% FBS (Cytiva, Marlborough, MA, USA). KEAP1 variant cells were generated by Zhao et al. as previously described (13). KEAP1 variant cells were maintained in MEM Alpha containing ribonucleosides, deoxyribonucleosides, phenol red, and l-glutamine, 1% penicillin/streptomycin (Cytiva, Marlborough, MA, USA), 10% FBS (Cytiva, Marlborough, MA, USA), and 1 μg/mL puromycin (Gibco, Waltham, MA, USA). HK-2 cells were obtained from ATCC (CRL-2190) and cultured in Dulbecco's Modified Eagle Medium (DMEM) (Corning, Tewksbury, MA, USA) with 1% penicillin/streptomycin and 10% FBS (Cytiva, Marlborough, MA, USA).

Unless otherwise noted, cells were seeded at a density of 1.5–2 × 10^5 cells per well in 6-well plates and allowed to proliferate overnight before treatment. For initial characterization of erythritol production from glucose and fructose, modified glucose-free DMEM (Hyclone, Logan, UT, USA) was prepared to contain 6.25, 12.5, or 25 mM glucose or 25 mM fructose. All further measurements (including knockdowns and metabolic assays) were performed in standard MEM Alpha or DMEM (5.5 mM glucose) with additional glucose, mannitol, or glycerol added to achieve desired concentrations of each carbohydrate. Cells were incubated with carbohydrates for 48 h, then polar metabolites were extracted, and relative cell number was measured by MTT.

Extraction and measurement of polar metabolites by GC-MS

Polar metabolites were extracted following the protocol for adherent cells by Sapcariu et al. (14). 10 μM $^{13}C_1$-ribitol (Cambridge isotope laboratories, Tewksbury, MA, USA) was added to methanol as an internal standard during extraction. Dried extracts were derivatized and metabolites

(erythritol, $^{13}C_1$-ribitol, and sorbitol) were measured by GC-MS as previously described (15). In SIM mode, mass spectra of erythritol (*m/z* 217), $^{13}C_1$-ribitol (*m/z* 218), and sorbitol (*m/z* 319) were acquired from 8 to 9, 10 to 11, and 12 to 13 min, respectively. Metabolite peaks were selected based on the retention time of their respective standards. Relative erythritol and sorbitol were calculated by dividing their absolute intensity by the absolute intensity of $^{13}C_1$-ribitol. Relative erythritol and sorbitol were then normalized to cell number, measured by MTT.

MTT assay for relative cell number

3-(4,5-dimethylthiazol-2-yl)-2,5-diphenyltetrazolium bromide (MTT) reagent (MP Bio, Santa Ana, CA, USA) dissolved in 1X PBS (5 mg/mL) was added to culture medium to a final concentration of 0.16 mg/mL. Cells were incubated for 4 h at 37°C, after which media and MTT reagent were removed. Formazan crystals were solubilized in 1 mL DMSO, diluted 1:10 in additional DMSO, then transferred to a microplate to quantify A_{570} using a Biotek plate reader.

Knockdown of sorbitol dehydrogenase, glucose-6-phosphate dehydrogenase, transketolase, and transaldolase using siRNA

Non-targeting control siRNA and siRNA targeting *SORD*, *G6PD*, *TKT*, and *TALDO* were purchased from Horizon Discovery. Product numbers and sequences are provided in **Supplementary Table 1**. A549 cells were reverse transfected using RNAiMAX (Thermo Fisher Scientific, Waltham, MA, USA) according to manufacturer's instructions. Per well (6-well plate), 2 μL of 20 μM siRNA and 5 μL RNAiMAX were diluted in 400 μL OptiMEM (Thermo Fisher Scientific), mixed gently and incubated for 20 min at room temperature. The solution was applied to the well 5 min prior cell seeding. 2×10^5 cells were seeded in 1,600 μL standard 5.5 mM glucose MEM Alpha or 25 mM glucose MEM Alpha. Transfected cells were incubated for 48 h until metabolite extraction or measurement of cell density by MTT.

Measurement of intracellular NADPH and metabolic phenotype

For measurement of NADPH or metabolic phenotype in 96-well plates, cells were transfected as described with reagents adjusted to a provide final volume of 200 μL per well: 0.1 μL siRNA, 0.25 μL RNAiMAX, and 20 μL OptiMEM, and 180 μL of culture medium.

NADPH was measured following reverse transfection using the NADP/NADPH-Glo^{TM} Assay (Promega, Madison, WI, USA). Briefly, 7×10^3 cells per well were reverse transfected with siRNA targeting control, *SORD,* or *G6PD* and incubated for 48 h in standard (5.5 mM glucose) or 25 mM glucose MEM Alpha. To measure NADPH individually, culture media was aspirated and replaced with 50 μL 1X PBS and 50 μL of 0.2 N NaOH with 1% DTAB to lyse cells. 50 μL of cell lysate was transferred to a white 96-well luminometer plate then incubated for 15 min at 60C followed by 10 min at room temperature. The base was neutralized with 50 μL Trizma/HCL, then NADPH was measured as described in the manufacturer's protocol.

Oxygen consumption rate (OCR) and extracellular acidification (ECAR) were measured using the Seahorse XF Cell Energy Phenotype Test Kit (Agilent, Santa Clara, CA, USA). 12×10^3 cells per well were reverse transfected with siRNA control or targeting *SORD* in a Seahorse XF24 Cell Culture Microplate (Agilent, Santa Clara, CA, USA) with MEM Alpha adjusted to 10 mM glucose. 10 mM glucose was chosen to match the Assay Buffer glucose concentration. After 48 h, baseline OCR and ECAR were measured following the manufacturer's protocol in Seahorse Assay Buffer (phenol red-free DMEM with 1 mM pyruvate, 2 mM glutamine, and 10 mM glucose).

Western blot analysis

Cells were lifted using 0.25% trypsin-EDTA, pelleted, and rinsed once with 1X PBS. Cell pellets were lysed by sonication in lysis buffer containing 15% NaCl, 5 mM EDTA (pH 8), 1% Triton X100, 10 mM Tris-Cl, 5 mM DTT, and 10 μL/mL protease inhibitor cocktail (Sigma Aldrich, St. Luis, MO, USA). Protein concentration was determined with a modified Lowry assay (16). Equal amounts of protein (15–25 μg) were loaded onto a 10% SDS gel and transferred to a PVDF membrane (Millipore Sigma, St. Luis, MO, USA). Membranes were blocked overnight at 4C in 5% non-fat milk, incubated in primary antibody overnight at 4C, then incubated with secondary antibody for 1 h at room temperature. Primary antibodies against alpha tubulin (ATUB), KEAP1, GAPDH, G6PD (Cell Signaling Technology, Danvers, MA, USA), SORD, TALDO, and TKT (ProteinTech, Rosemont, IL, USA) were diluted 1:1,000. Secondary anti-rabbit and anti-mouse antibodies were diluted 1:50,000 (Thermo Fisher Scientific, Waltham, MA, USA). After antibody incubation, blots were imaged using a Protein Simple FluorChem E with Clarity Western ECL Substrate (Bio-Rad, Hercules, CA, USA). Band intensity was measured using ImageJ (NIH, Bethesda, MA, USA).

^{13}C-glucose tracing

To measure the incorporation of labeled glucose in endogenous erythritol, modified glucose-free DMEM (Hyclone,

10.3389/fnut.2022.953056

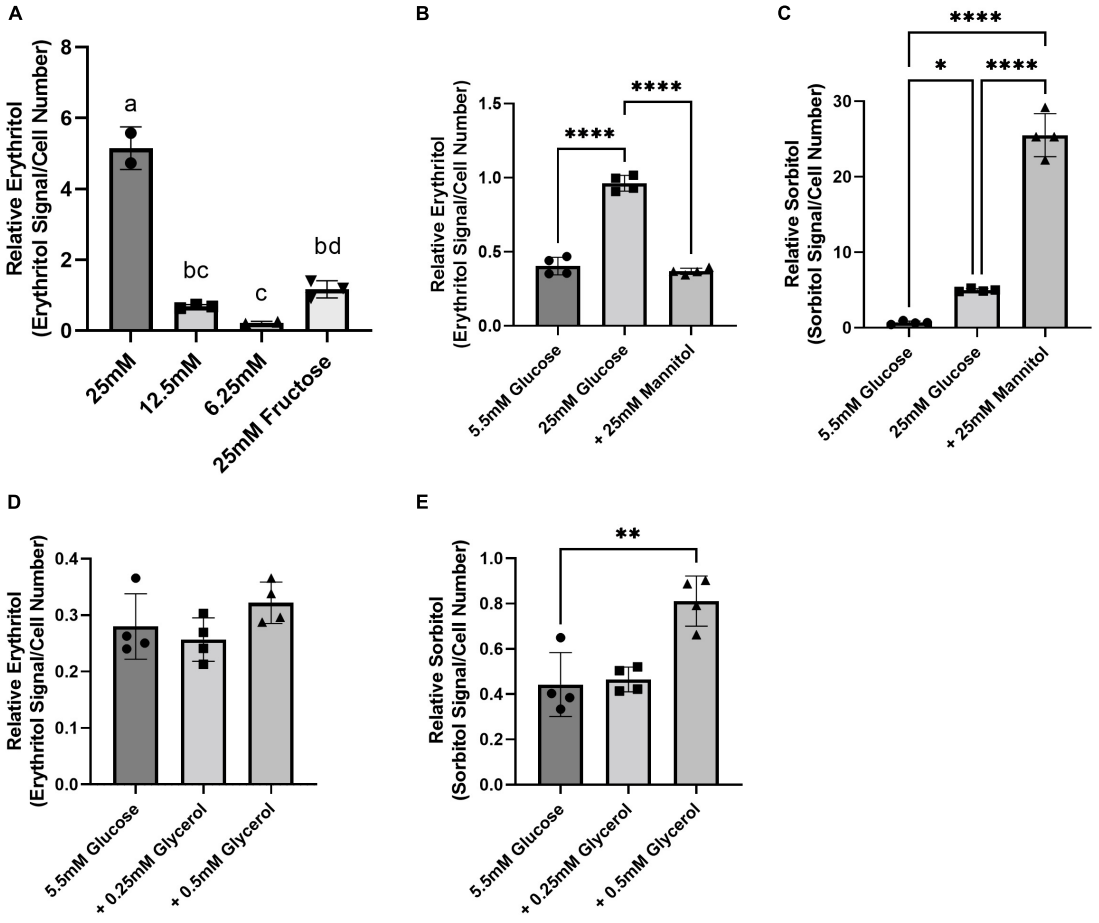

FIGURE 1
Intracellular erythritol and sorbitol levels respond to carbohydrate concentrations in media and osmotic stress. **(A)** Relative erythritol in cells cultured for 48 h in media containing 25, 12.5, or 6.25 mM glucose or 25 mM fructose. Labeled means without a common letter differ, $p < 0.05$. **(B)** Relative erythritol and **(C)** relative sorbitol in cells cultured in media containing 5.5 or 25 mM glucose, or 5.5 mM glucose supplemented with 25 mM mannitol. **(D)** Relative erythritol and **(E)** relative sorbitol in cells cultured in 5.5 mM glucose media or 5.5 mM glucose media containing 0.25 or 0.5 mM glycerol. All relative metabolite values are normalized to internal standard and cell number. Data are shown as mean ± SD and were analyzed by one-way ANOVA, followed by Tukey's multiple comparisons test ($n = 2–4$). $^{*}p < 0.05$, $^{**}p < 0.01$, $^{****}p < 0.0001$.

Logan, UT, USA) was adjusted to 25 mM glucose with either 1-[^{13}C]-glucose or 6-[^{13}C]-glucose (Cambridge isotope laboratories, Tewksbury, MA, USA). Cells were reverse transfected as described above, incubated with labeled glucose for 48 h, then polar metabolites were harvested and measured by GCMS. The mass spectra were acquired for erythritol from *m/z* 320 (M0) to *m/z* 324 (M4). Mass isotope distribution was calculated as previously described (6).

Treatment with hydrogen peroxide

Cells were seeded at 2×10^5 cells per well in 6-well plates and allowed to proliferate overnight. The following day, cells were treated with water or hydrogen peroxide ranging from 150 to 600 μM hydrogen peroxide for either 6 or 8 h. After treatment, polar metabolites and relative cell number were measured. The percentage of live cells was determined using trypan blue staining quantified using a TC10 Automated Cell Counter (Bio-Rad, Hercules, CA, USA). To determine intracellular NADPH and oxidized glutathione (GSSG), 7×10^3 cells/well in a 96-well plate were treated with hydrogen peroxide, then NADPH was measured as described above. GSSG was measured using the GSH/GSSG-Glo assay (Promega, Madison, WI, USA) per the manufacturer's protocol.

Statistical analysis

All statistical analyses were conducted in GraphPad Prism 9 (GraphPad Software, San Diego, CA, USA). All data are shown as mean ± SD, and *p*-values lower than 0.05 were considered statistically significant. Comparisons between two groups were analyzed by unpaired *t*-test. Comparisons between more than

10.3389/fnut.2022.953056

two groups were analyzed by one-way ANOVA followed by Tukey's multiple comparisons test or two-way ANOVA with Sidak's or Tukey's multiple comparisons test.

Results

Intracellular erythritol increases in response to glucose and fructose in culture medium

A549 cells were used to assess the contribution of substrate availability to erythritol synthesis given their robust PPP activity and known ability to generate erythritol (7). As expected, intracellular erythritol was significantly higher in A549 cells cultured in 25 mM glucose compared to 6.25 mM glucose (**Figure 1A**, $p < 0.0001$). 25 mM glucose was chosen to model hyperglycemia. In the absence of glucose, 25 mM fructose also significantly increased erythritol compared to the 6.25 mM glucose control (**Figure 1A**, $p < 0.05$). Treatment with 25 mM mannitol was performed as a control for the osmotic stress induced by high-glucose (25 mM) media. Mannitol treatment did not significantly increase intracellular erythritol compared to 5.5 mM glucose controls (**Figure 1B**). Sorbitol accumulation is one mechanism of responding to hyperosmolarity (17). Measurement of intracellular sorbitol confirmed the strong induction of osmotic stress in mannitol-treated cells. Mannitol elevated sorbitol nearly 40-fold above 5.5 mM glucose and fivefold above 25 mM glucose-treated cells (**Figure 1C**, $p < 0.0001$). Sorbitol accumulation was also modestly induced by 25 mM glucose compared to control media, as expected due to increased flux through the polyol pathway as a result of increased glucose (**Figure 1C**, $p < 0.05$) (17).

We also evaluated the effect of exposure to excess glycerol, which acts as both an osmolyte and an alternative carbon source, on erythritol synthesis. There was no significant difference in erythritol content in cells treated with 5.5 mM glucose and 5.5 mM glucose media containing 0.25 or 0.5 mM glycerol (**Figure 1D**). In contrast, sorbitol was significantly higher in cells treated with 0.5 mM glycerol compared to control cells (**Figure 1E**, $p < 0.01$).

We have previously demonstrated that in mice, the liver and kidney are primary contributors to endogenous erythritol synthesis (15). We therefore repeated exposure to 5.5 or 25 mM glucose media in HK-2 cells, a human proximal tubular cell line derived from normal kidney cells. High glucose media caused a 40% increase in erythritol in HK-2 cells (**Figure 2**, $p < 0.001$). Collectively, these findings demonstrate that erythritol synthesis is elevated in response to glucose availability and not because of osmotic stress.

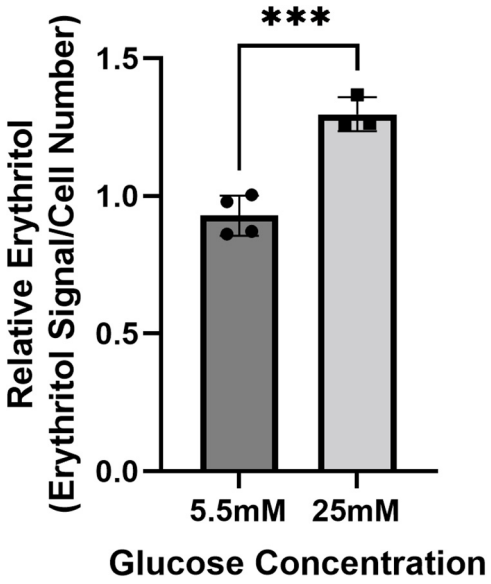

FIGURE 2
Intracellular erythritol in HK-2 cells is increased in high-glucose media. Intracellular erythritol was measured in HK-2 cells exposed to 5.5 or 25 mM glucose media for 48 h ($n = 4$). Data is normalized by internal standard and cell number, shown as mean ± SD, and analyzed by unpaired *t*-test. ***$p < 0.001$.

Reduction of sorbitol dehydrogenase decreases erythritol synthesis and NADPH availability

As previously described, erythritol is synthesized from glucose through the PPP in mammalian cells (6, 7). To determine the rate-limiting step in erythritol synthesis, we reduced expression of SORD and G6PD using siRNA. G6PD is generally considered the rate-limiting enzyme of the PPP. Unexpectedly, we found that in 5.5 mM glucose media, reduction of neither enzyme affected intracellular erythritol levels (**Figure 3A**). Knockdown of SORD and G6PD were validated by western blot (**Figure 3B**). When exposed to 25 mM glucose media, siControl and siG6PD cells both had significantly higher erythritol compared to cells cultured in 5.5 mM glucose (**Figure 3A**, $p < 0.001$ and $p < 0.0001$, respectively). siSORD cells did have reduced intracellular erythritol in response to hyperglycemia (**Figure 3A**), consistent with previous findings (7). These data demonstrate that, in A549 cells, erythritol synthesis is limited by *SORD* expression but not by *G6PD* expression in response to high-glucose culture medium.

Erythritol synthesis uses the coenzyme NADPH, which is produced by G6PD during the first steps of the PPP. We found that in both 5.5 and 25 mM glucose media, siG6PD significantly reduced intracellular NADPH compared to siControl and siSORD treated cells (**Figure 3C**, $p < 0.001$). SORD knockdown did not significantly modify NADPH compared to control cells

at either glucose concentration (Figure 3C). Taken together, these findings suggest that erythritol synthesis is not affected by changes in intracellular NADPH.

We also assessed the effect of siSORD on cellular energy metabolism using real-time cell metabolic analysis (i.e., Agilent Seahorse technology, Santa Clara, CA, USA). SORD knockdown significantly increased extracellular acidification rate (ECAR) (Figure 3D, $p < 0.01$) and did not significantly change the oxygen consumption rate (OCR) (Figure 3D). The increase in ECAR without significant changes to OCR likely indicates that when SORD expression is reduced, glycolysis and subsequent secretion of lactate are elevated.

Knockdown of the non-oxidative pentose phosphate pathway enzyme transketolase reduces erythritol synthesis

The PPP consists of an oxidative phase, for which G6PD is rate-limiting, and a non-oxidative phase. The non-oxidative PPP, which provides erythrose (via erythrose-4-phosphate) for erythritol synthesis, requires the activities of transketolase (TKT) and transaldolase (TALDO) enzymes. Indeed, knockdown of TKT expression in cell cultured in high-glucose media significantly reduced intracellular erythritol levels (Figure 4A, $p < 0.01$). This decrease in erythritol was of the same magnitude as siSORD (Figure 4A, $p < 0.01$). Reduction of TALDO, however, did not significantly reduce intracellular erythritol compared to siControl cells (Figure 4A). Successful knockdown of these enzymes was validated by western blot (Figures 4B,C).

Given the effect of increasing glucose in media on erythritol synthesis, we assessed if high glucose also effected SORD and TKT expression. We found no significant difference SORD or TKT expression between 5.5 and 25 mM glucose-treated cells (Figures 5A,B).

Glucose-derived erythritol carbons originate from the pentose phosphate pathway

We used position-specific [^{13}C]-glucose tracing to determine if carbons for erythritol synthesis must first pass through the oxidative PPP, or can be derived directly from glycolysis through fructose-6-phosphate and glyceraldehyde-3-phosphate catalyzed by TKT and TALDO (Figure 6A). 1-[^{13}C]-glucose would be incorporated into erythritol through glycolysis, whereas 6-[^{13}C]-glucose is incorporated through the PPP (Figure 6A). We found that in cells treated with 1-[^{13}C]-glucose, incorporation of labeled carbons into erythritol was 0% (M1 erythritol) (Figure 6B). Contrastingly, treatment with 6-[^{13}C]-glucose in siControl cells resulted in 60% M1 erythritol incorporation (Figure 6C). Treatment with siSORD or siTKT also significantly reduced incorporation of 6-[^{13}C]-glucose carbons into M1 erythritol (Figure 6C, $p < 0.0001$ and $p < 0.05$). Consistent with previous findings, under high glucose conditions all erythritol carbons are derived from the oxidative PPP, but erythritol synthesis is limited by the enzymes SORD and TKT in the non-oxidative PPP (6, 7).

Oxidative stress induces erythritol synthesis

We found that treatment with hydrogen peroxide for 8 h significantly increased intracellular erythritol without significantly decreasing the percentage of live cells (Figure 7A, $p < 0.0001$, and Figure 7B). As expected, hydrogen peroxide also caused a significant increase in oxidized glutathione (Figure 7C, $p < 0.0001$) and reduction in intracellular NADPH (Figure 7D, $p < 0.01$). These findings suggest that erythritol synthesis is increased in response to oxidative stress and support the previous observation that decreased NADPH levels do not affect erythritol synthesis capacity (Figure 3C).

Keap1 mutations alter response to glucose and oxidative stress

We hypothesized that the increase in intracellular erythritol in response to high glucose and oxidative stress may be mediated by NRF2. To test this hypothesis, we utilized A549 cells that stably express either ectopic wildtype (WT) KEAP1 or the cysteine-to-serine mutations C273S and C151S (13, 18). The mutation C273S impairs the ability of KEAP1 to repress NRF2, resulting in constitutively active NRF2. C151S results in constitutive repression of NRF2 (18).

We confirmed that the A549 KEAP1 mutants differentially express KEAP1 and G6PD, a downstream target of NRF2 (Figures 8A,B). Cells expressing WT, C151S, and C273S all significantly increase intracellular erythritol in 25 mM glucose media (Figure 9A, $p < 0.001$). The magnitude of this response, however, differed by KEAP1 status: C273S cells had 2 and 3-fold higher erythritol in 25 mM glucose media compared to WT and C151S-expressing cells (Figure 9A). This finding indicates that constitutively active NRF2 results in the most robust increase in erythritol synthesis from exposure to high-glucose in culture medium. We found a similar pattern in intracellular sorbitol. All cells responded to 25 mM glucose by increasing sorbitol (Figure 9B, $p < 0.0001$), but C273S cells accumulated twofold more sorbitol than cells with lower NRF2 expression.

Treatment with 300 μM hydrogen peroxide for 5 h elevated erythritol in KEAP1 WT and C151S cells (Figure 9C, $p < 0.0001$). There was no difference in C273S cells (Figure 9C).

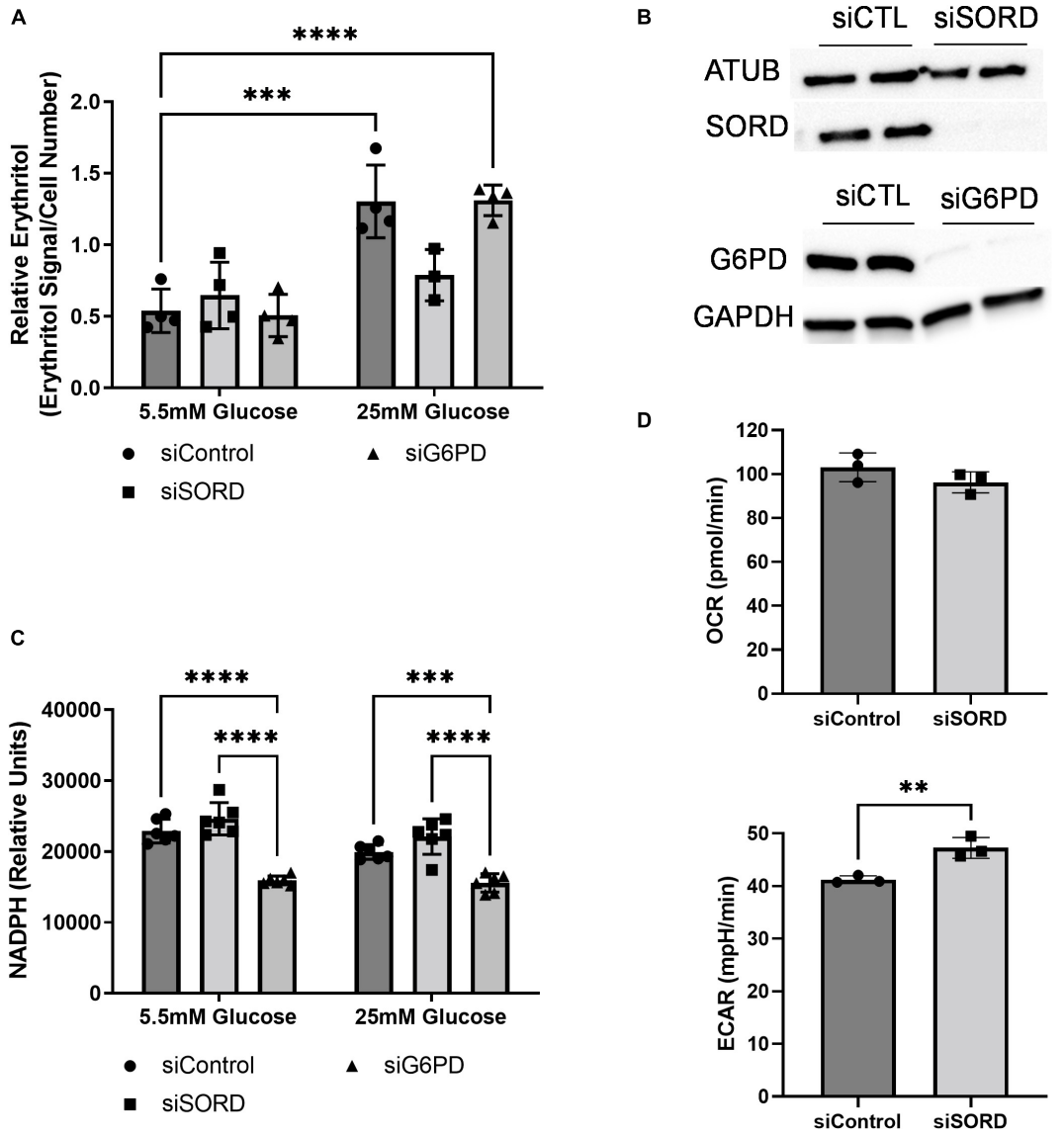

FIGURE 3
SORD and G6PD knockdown affect cellular metabolism. Knockdown of SORD and G6PD were performed by reverse transfection. **(A)** Intracellular erythritol (n = 4), **(B)** protein levels of SORD and G6PD, and **(C)** intracellular NADPH were measured after 48 h treatment with 5.5 or 25 mM glucose (n = 6). Erythritol was normalized to internal standard and cell number. **(D)** OCR and ECAR were measured in control or SORD knockdown cells following 48 h in 10 mM glucose media and normalized to cell number (n = 3). Data is presented as mean ± SD, **(A,C)** were analyzed by two-way ANOVA followed by Sidak's multiple comparisons test, **(D)** was analyzed with an unpaired t-test. $^{**}p < 0.01$, $^{***}p < 0.001$, $^{****}p < 0.0001$. ATUB, alpha tubulin; ECAR, extracellular acidification rate; GAPDH, glyceraldehyde 3-phosphate dehydrogenase; G6PD, glucose 6-phoshate dehydrogenase; SORD, sorbitol dehydrogenase.

Oxidized glutathione was also significantly elevated in KEAP1 WT and C151S, but not C273S cells (Figure 9E, $p < 0.05$). Importantly, treatment with 600 μM hydrogen peroxide caused significant cell death in KEAP1 WT and C151S cells, indicating impaired response to oxidative stress in cells with reduced NRF2 activity. This finding is supported by the relative resistance of the C273S cells, which have constitutively active NRF2. Intracellular sorbitol also increased in response to 300 μM hydrogen peroxide in all 3 cell types, which indicates an accumulation of intracellular glucose (Figure 9D, $p < 0.05$) and possible inhibition of glycolysis under these conditions.

Discussion

Previous literature has identified that, in mammals, erythritol is synthesized from glucose through the PPP (6). Erythritol synthesis from erythrose can be catalyzed by SORD

10.3389/fnut.2022.953056

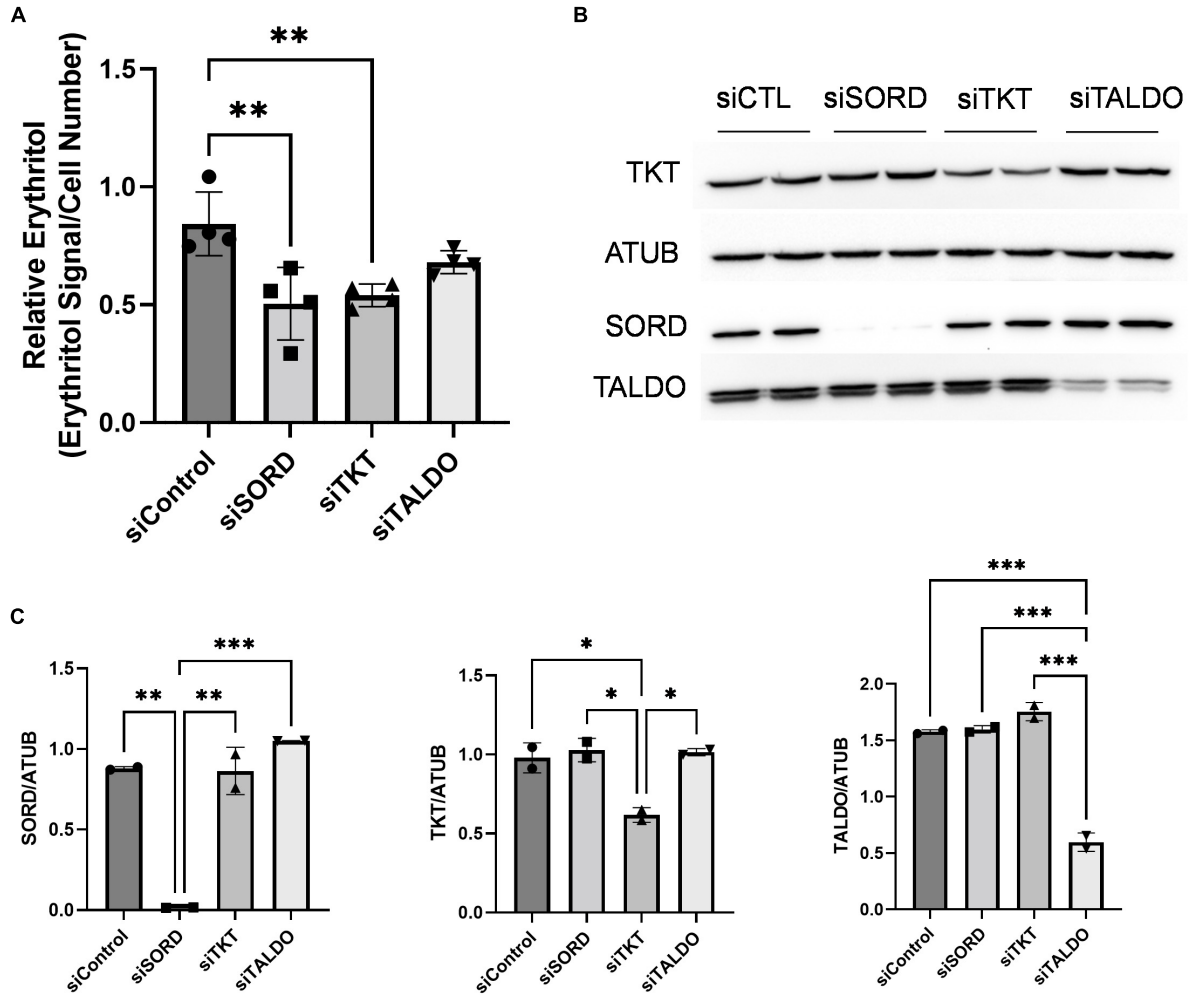

FIGURE 4
Knockdown of non-oxidative PPP enzymes SORD and TKT decrease intracellular erythritol levels. Knockdown of SORD, TKT, and TALDO were performed using reverse transfection. After 48 h treatment with 25 mM glucose media, **(A)** intracellular erythritol (n = 4) and **(B)** protein expression was measured. **(C)** Protein expression was quantified using Image J (n = 2). Relative erythritol is normalized to internal standard and cell number. Data is shown as mean ± SD and was analyzed by ordinary one-way ANOVA and Tukey's multiple comparisons test. *$p < 0.05$, **$p < 0.01$, ***$p < 0.001$. ATUB, alpha tubulin; CTL, control; SORD, sorbitol dehydrogenase; TALDO, transaldolase; TKT, transketolase.

and ADH1 using NADPH as a cofactor (7). The precursor of erythrose is erythrose-4-phosphate, which is a product of the non-oxidative PPP. The regulation of erythritol synthesis and its role in metabolic homeostasis, however, is poorly understood (19). Here, we demonstrate that erythritol synthesis is modulated both by glucose availability and oxidative stress in A549 cells. We observed that intracellular erythritol increased dose-dependently with increasing glucose in culture media (**Figure 1A**). Interestingly, we also demonstrated that in the absence of glucose, erythritol synthesis is still elevated by exposure to 25 mM fructose compared to 6.25 mM glucose (**Figure 1A**). This elevation is modest, however, when compared to the response to 25 mM glucose media. In A549 cells, fructose is converted to glycolytic intermediates that are primarily used for fatty acid synthesis (20, 21). Fatty acid oxidation utilizes NADPH, thus increasing the demand for NADPH regeneration in the oxidative PPP (21). Fructose, then, may promote erythritol synthesis directly through increased glycolytic intermediates or through increased PPP flux.

In addition to increased nutrient availability, excess carbohydrates are a source of osmotic stress in cell culture. In yeast, erythritol synthesis can be induced by osmotic stress (22). In humans, the 6-carbon polyol sorbitol is also known to be elevated during osmotic stress (17, 23). To evaluate if erythritol synthesis is an additional mechanism of osmoregulation, we treated cells with mannitol. Mannitol is strong osmolyte that undergoes little metabolism in humans (24). Interestingly, mannitol treatment did not affect intracellular erythritol, whereas sorbitol was significantly elevated (**Figures 1B,C**). This may be explained by differing capacities for diffusion across

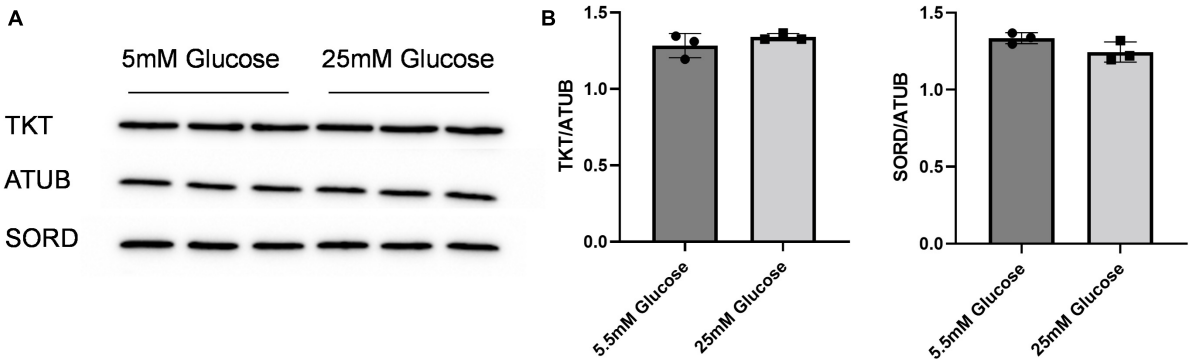

FIGURE 5
SORD and TKT protein expression do not increase in response to high glucose media. **(A)** Western blot of TKT and SORD expression after 48 h treatment in 5.5 mM or 25 mM glucose media and **(B)** quantification. Expression was quantified with ImageJ (n = 3). ATUB, alpha tubulin; SORD, sorbitol dehydrogenase; TKT, transketolase.

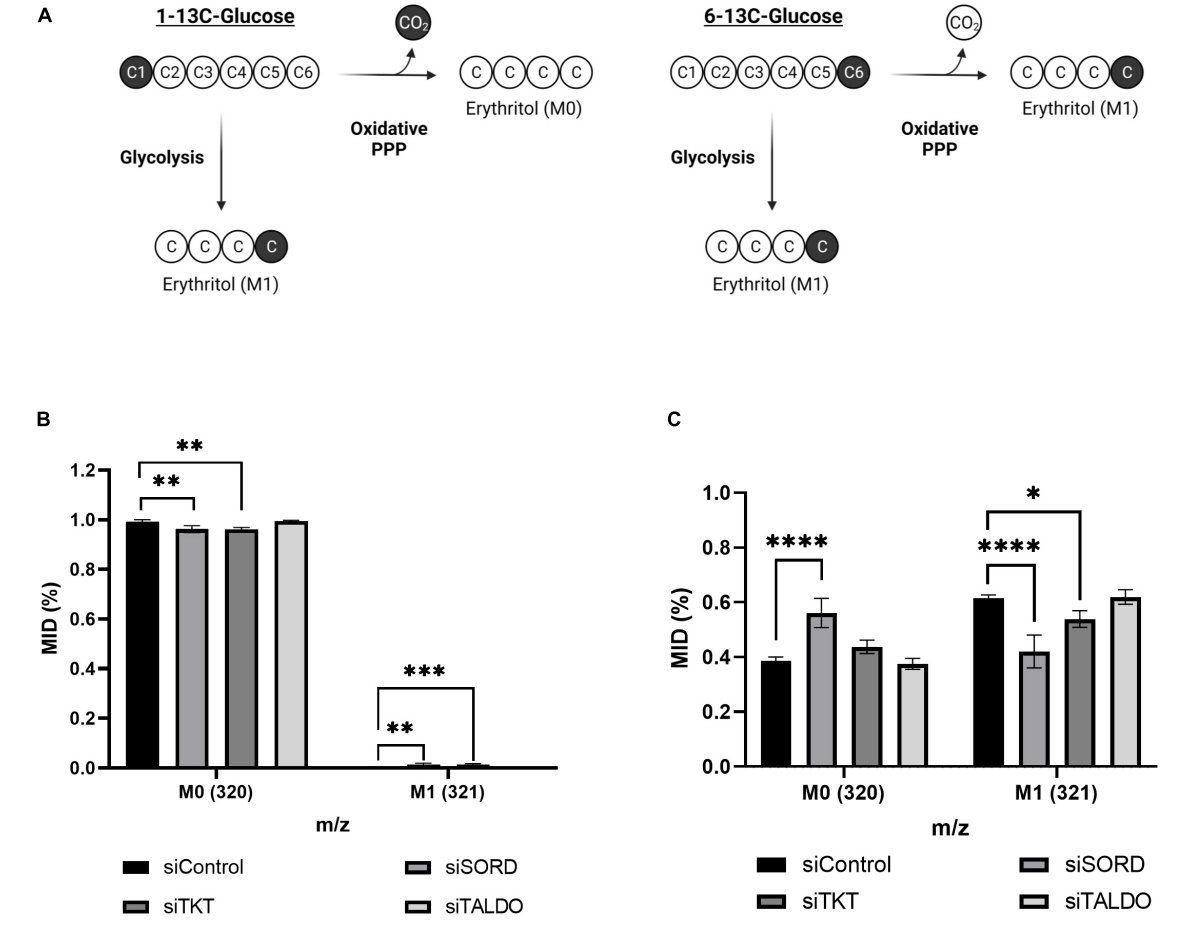

FIGURE 6
Erythritol carbons are derived from the oxidative PPP, not directly from glycolysis. **(A)** Representation of differential incorporation of ^{13}C into erythritol from 1-[^{13}C] or 6-[^{13}C]-glucose. **(B)** MID of unlabeled (M0) and labeled (M1) erythritol after incubation with 25 mM 1-[^{13}C]-glucose. **(C)** MID of unlabeled (M0) and labeled (M1) erythritol after incubation with 25 mM 6-[^{13}C]-glucose. Data is shown as mean ± SD, n = 4–5, and was analyzed by two-way ANOVA with Dunnett's multiple comparisons test. *$p < 0.05$, **$p < 0.01$, ***$p < 0.001$, ****$p < 0.0001$. ATUB, alpha tubulin; MID, mass isotope distribution; SORD, sorbitol dehydrogenase; TALDO, transaldolase; TKT, transketolase.

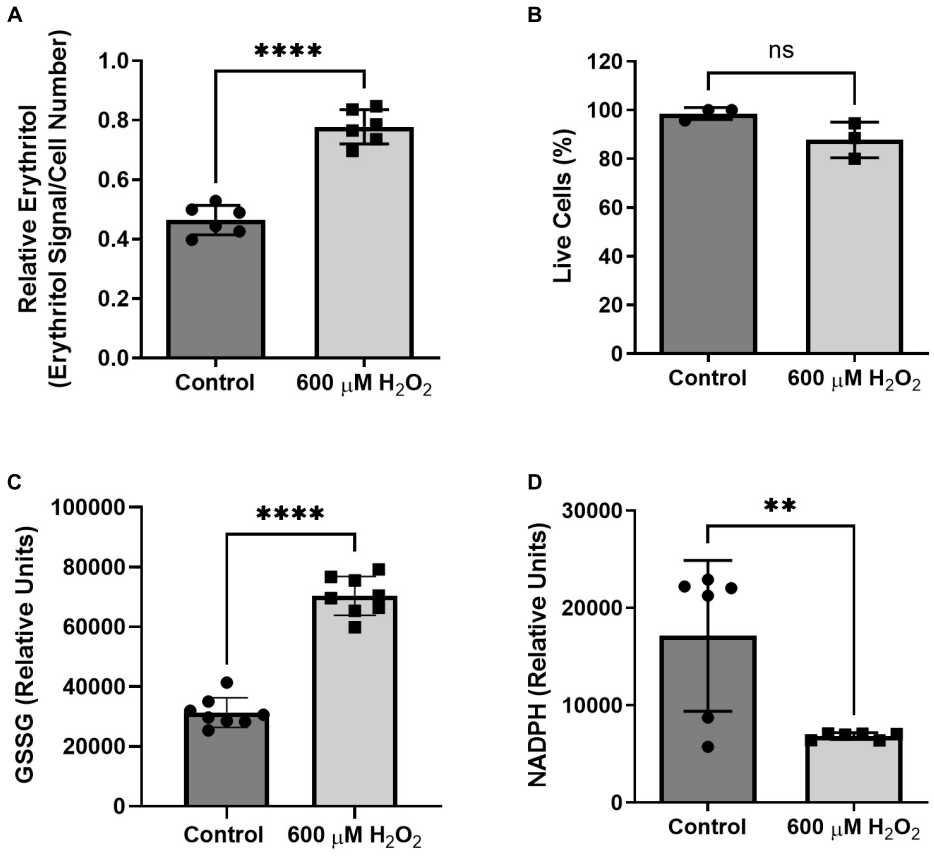

FIGURE 7
Intracellular erythritol and NADPH respond to hydrogen peroxide in culture medium. Cells were exposed to 600 μM hydrogen peroxide or vehicle for 8 h, after which **(A)** intracellular erythritol, **(B)** percentage of live cells, **(C)** oxidized glutathione (GSSG), and **(D)** NADPH were measured. Erythritol is normalized to internal standard and cell number. Data is presented as mean ± SD, n = 3–6, analyzed by unpaired t-test. $^{**}p < 0.01$, $^{****}p < 0.0001$. GSSG, oxidized glutathione; H_2O_2, hydrogen peroxide.

the plasma membrane. Erythritol more readily diffuses across cell membranes than the larger polyol sorbitol (24). Sorbitol, therefore, is likely a more effective endogenous osmolyte to combat hyperosmotic stress than is erythritol.

Yeast also use glycerol as a substrate for erythritol synthesis by converting glycerol to glyceraldehyde-3-phosphate, a precursor of erythrose-4-phosphate in the non-oxidative PPP (22). Based on the finding that fructose, another direct precursor of erythrose-4-phosphate, elevated erythritol, we expected that glycerol treatment would produce similar results in human cells. In further support that erythritol does not respond to osmotic stress in human cells, 0.5 mM glycerol significantly increased intracellular sorbitol, but did not impact intracellular erythritol (**Figures 1D,E**). Collectively, these data support that erythritol is produced in response to carbohydrate abundance and not in response to osmotic stress.

A549 cells are derived from cancerous tissue, which is one limitation of this work. due to the divergent utilization of glucose compared to non-cancerous cells. In cancer cells the Warburg effect results in increased glucose uptake and glycolysis (25). In addition, A549 cells are known to have high PPP activity, which sustains NADPH and nucleic acid synthesis in these rapidly dividing cells but could also make erythritol synthesis more pronounced (11, 12). Due to these metabolic differences, we aimed to validate the key finding that intracellular erythritol is proportional to glucose availability in a different cell model. We chose to use HK-2 cells based on our previous work showing that the kidney contains relatively high endogenous erythritol in mice (15). Indeed, we found that HK-2 cells also respond to excess glucose with an increase in intracellular erythritol (**Figure 2**), consistent with previous observations of increased PPP flux in HK-2 cells cultured in hyperglycemic hypoxic conditions (26). This demonstrates that glucose availability can also regulate synthesis in cells derived from different erythritol-synthesizing tissues.

Our work validated the previous finding in A549 cells that SORD knockdown significantly decreases erythritol synthesis (7), as previous experiments were conducted in media containing 25 mM glucose (7). This is the first study to report that the effect of SORD knockdown on intracellular erythritol

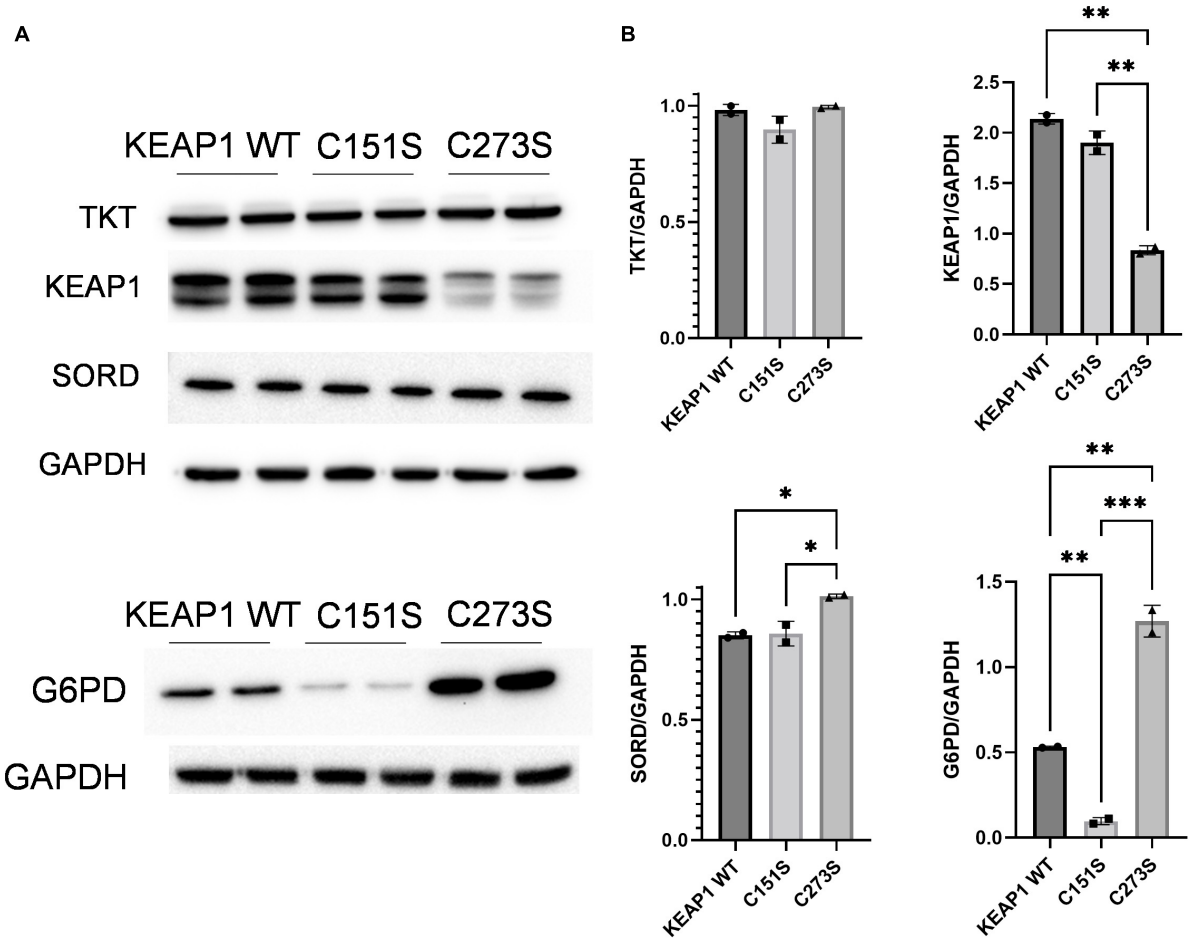

FIGURE 8
KEAP1 variants have modified expression of proteins regulated by NRF2. **(A)** Western blots of TKT, KEAP1, SORD, and G6PD expression in KEAP1 mutant cells and **(B)** quantification of protein expression. Expression was quantified with ImageJ ($n = 3$). G6PD, glucose-6-phosphate dehydrogenase; GAPDH, glyceraldehyde-3-phosphate dehydrogenase; KEAP1, Kelch Like ECH Associated Protein 1; SORD, sorbitol dehydrogenase; TKT, transketolase. $^{*}p < 0.05$, $^{**}p < 0.01$, $^{***}p < 0.001$.

is dependent on glucose level. In basal glucose media (5.5 mM), siSORD does not significantly decrease intracellular erythritol whereas in high glucose media (25 mM glucose), siSORD caused a 40% reduction (**Figure 3A**). This further supports the primary role of glucose availability in the synthesis of erythritol.

G6PD is generally regarded as the rate-limiting enzyme of the PPP (27). We expected, then, that knockdown of G6PD would result in reduced intracellular erythritol in high-glucose media. Interestingly, G6PD knockdown did not blunt the glucose-induced increase in erythritol (**Figure 3A**). This is likely due to the alternative enzyme hexose-6-phosphate dehydrogenase (H6PD). H6PD is an endoplasmic reticulum enzyme capable of catalyzing the same conversion of glucose-6-phosphate to 6-phosphogluconate as G6PD (28). In A549 cells, knockdown of either G6PD or H6PD reduced, but did not eliminate synthesis of D-ribose, the product of the non-oxidative PPP (28). This suggests that when the first step of the PPP is reduced, there is still adequate flux through the non-oxidative PPP to sustain erythritol synthesis. This is further supported by the finding that in melanoma cells (which also have high PPP activity), when G6PD function was impaired, there was no reduction in erythrose-4-phosphate levels (29). These studies demonstrate that cancer cells are resilient to G6PD inhibition and continue to fuel the non-oxidative PPP and, subsequently, erythritol synthesis.

We next evaluated the impact of knocking down the downstream non-oxidative PPP enzymes TKT and TALDO. We found that knocking down *TKT*, but not *TALDO*, reduced erythritol in 25 mM glucose media by a similar magnitude as *SORD* knockdown (**Figure 4A**). This is consistent with historic reports that *TALDO* deficiency resulted in accumulation, rather than depletion, of erythritol and other polyols in plasma and urine (30, 31). Our findings indicate that both *SORD* and *TKT* expression are essential for the synthesis of erythritol.

10.3389/fnut.2022.953056

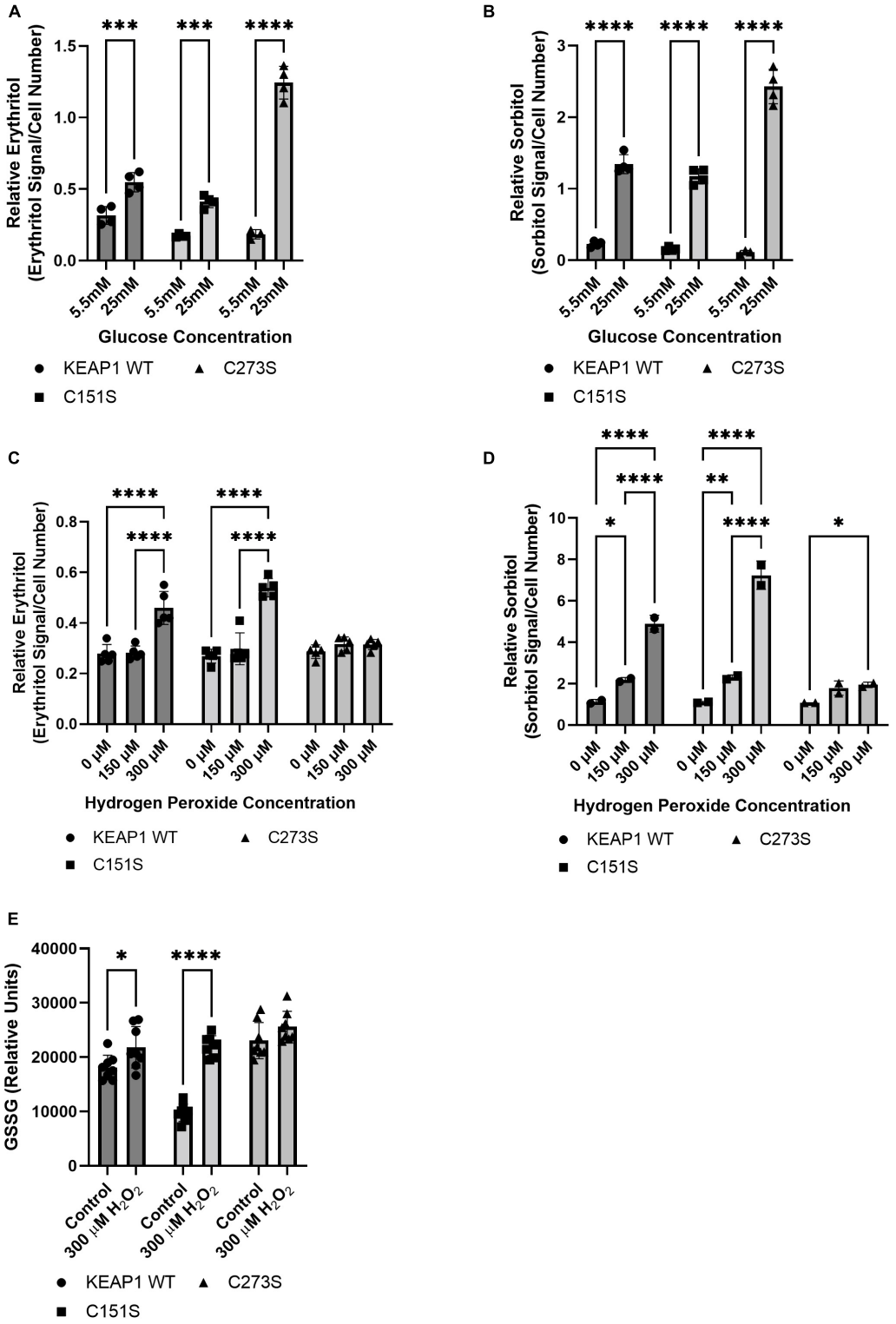

FIGURE 9

KEAP1 variants modulate response to high glucose and oxidative stress. Intracellular erythritol **(A)** and sorbitol **(B)** in KEAP1 variant cells following 48 h treatment with 5.5 mM or 25 mM glucose (n = 4). Erythritol **(C)** and sorbitol **(D)** following exposure to 0–300 μM hydrogen peroxide for 5 h (n = 2–5). **(E)** Oxidized glutathione following 5 h treatment with hydrogen peroxide. Erythritol is normalized to internal standard and cell number. Data is presented as mean ± SD and analyzed by two-way ANOVA followed by Sidak's **(A,B,E)** and Tukey's **(C,D)** multiple comparisons test. *$p < 0.05$, **$p < 0.01$, ***$p < 0.001$, ****$p < 0.0001$. WT-KEAP1 cells stably overexpress KEAP1. C273S cells have impaired ability of KEAP1 to repress NRF2, resulting in constitutively active NRF2. C151S cells exhibit constitutive repression of NRF2. GSSG, oxidized glutathione; H_2O_2, hydrogen peroxide.

As previously discussed, the non-oxidative PPP is critical to supply ribose-5-phosphate for nucleic acid synthesis in A549 cells. Additional characterization in non-transformed tissues will shed further light on the regulatory role of TKT in erythritol synthesis; these experiments are ongoing in mouse models.

TKT participates in two reversible sugar conversions in the non-oxidative PPP. The TKT-catalyzed reaction erythrose-4-phosphate + xylulose-5-phosphate ↔ fructose-6-phosphate + glyceraldehyde-3-phosphate is a bridge by which carbons can be passed between glycolysis and the PPP. Because siG6PD did not limit erythritol synthesis, but siTKT did, we aimed to understand if erythritol synthesis is being supported by carbons directly from glycolytic intermediates when glucose availability is high. We found using position-specific [^{13}C]-glucose tracing that when G6PD expression is not altered, glucose passes through the oxidative PPP before incorporation into erythritol (**Figures 6A–C**). This is in agreement with the previous finding that in A549 cells, all erythritol was derived from glucose passed through the oxidative PPP (6).

Flux through the PPP is a key defense mechanism to combat oxidative stress, primarily through generation of reducing equivalents as NADPH. We hypothesized that oxidative stress, therefore, would also elevate synthesis of erythritol. As expected, we found that intracellular erythritol is elevated in A549 cells exposed to hydrogen peroxide (**Figure 7A**). Interestingly, erythritol synthesis capacity is not associated with intracellular NADPH levels—in fact, erythritol was elevated with hydrogen peroxide treatment when NADPH was depleted (**Figure 7D**). Similarly, G6PD knockdown depleted intracellular NADPH, but did not affect erythritol levels (**Figure 3C**). Together, these findings suggest that flux of glucose through G6PD and intracellular NADPH are sufficient, even when NADPH is reduced, to support erythritol synthesis.

We further explored the relationship between oxidative stress and erythritol utilizing A549 *KEAP1* mutant cells with altered activity of NRF2 (13, 18). NRF2 directs glucose flux through the PPP by modifying enzyme expression (32, 33). We found that constitutively active NRF2 intensified glucose-induced erythritol synthesis, resulting in even higher erythritol levels than cells with normal or impaired NRF2 (**Figure 9A**). Notably, cells with constitutively active NRF2 did not have higher intracellular erythritol at baseline. This suggests that the co-occurrence of hyperglycemia and oxidative stress may be a key factor in elevating erythritol synthesis.

We also found that impairing NRF2 did not eliminate erythritol synthesis during oxidative stress but did lower the threshold for this response. In parental A549 cells, 600 μM hydrogen peroxide induced oxidative stress and elevated intracellular erythritol (**Figure 7A**). This dose was highly cytotoxic to cells with ectopic WT KEAP1 or the NRF2-repressing C151S mutation. WT KEAP1 and C151S cells increased erythritol synthesis following treatment with half the dose, 300 μM hydrogen peroxide (**Figure 9C**). Erythritol synthesis during oxidative stress may be due to both NRF2-dependent and NRF2-independent mechanisms. Oxidative stress inhibits the activity of several glycolytic enzymes through mechanisms that are not dependent on NRF2, promoting the accumulation of glycolytic intermediates (11, 12). We also observed significant accumulation of sorbitol in KEAP1 WT and C151S cells under oxidative stress (**Figure 9D**). This supports that intracellular glucose is elevated, likely due to the inhibition of glycolytic enzymes, which promotes alternative pathways (i.e., sorbitol and erythritol synthesis through the polyol and PPP, respectively). Overall, our findings in KEAP1 mutant cells further indicate that elevated erythritol synthesis is a marker of glucose flux through the PPP. In humans, elevated circulating erythritol is a predictive biomarker of cardiometabolic diseases (19). We demonstrated that erythritol is elevated by both hyperglycemia and oxidative stress in lung carcinoma cells, and that these effects can compound to further promote erythritol synthesis. Further research characterizing whole-body erythritol homeostasis and erythritol synthesis in non-transformed cells and/or tissues may provide a powerful tool for detecting early cardiometabolic dysfunction.

Data availability statement

The raw data supporting the conclusions of this article will be made available by the authors, without undue reservation.

Author contributions

SO, KH, and MF designed research. SO conducted research and analyzed data. AH assisted with methodology and software for analysis of mass isotope distribution. SO and MF wrote the manuscript. MF had primary responsibility for final content. All authors have read and approved the final manuscript.

Funding

This work was supported by the Hatch Federal Capacity Funds (grant no. 7000420) from the USDA National Institute of Food and Agriculture to MF. This work was supported by the Education and Workforce Development Predoctoral Fellowship (grant no. 2021-67034-35110/project accession no. 1026400) from the USDA National Institute of Food and Agriculture to

SO. AH was supported by the Federal State of Lower Saxony, Niedersächsisches Vorab (VWZN3266).

Acknowledgments

We are grateful to Christian Metallo for the generous gift of the A549 KEAP1 over-expression cell lines (WT and mutants).

Conflict of interest

The authors declare that the research was conducted in the absence of any commercial or financial relationships that could be construed as a potential conflict of interest.

Publisher's note

Supplementary material

The Supplementary Material for this article can be found online at: https://www.frontiersin.org/articles/10.3389/fnut.2022.953056/full#supplementary-material

References

1. Wang Z, Zhu C, Nambi V, Morrison AC, Folsom AR, Ballantyne CM, et al. Metabolomic pattern predicts incident coronary heart disease: findings from the atherosclerosis risk in communities study. *Arterioscler Thromb Vasc Biol.* (2019) 39:1475–82.

2. Rebholz CM, Yu B, Zheng Z, Chang P, Tin A, Köttgen A, et al. Serum metabolomic profile of incident diabetes. *Diabetologia.* (2018) 61:1046–54.

3. Shao M, Lu H, Yang M, Liu Y, Yin P, Li G, et al. Serum and urine metabolomics reveal potential biomarkers of T2DM patients with nephropathy. *Ann Transl Med.* (2020) 8:199–199. doi: 10.21037/atm.2020.01.42

4. Chen L, Cheng CY, Choi H, Ikram MK, Sabanayagam C, Tan GSW, et al. Plasma metabonomic profiling of diabetic retinopathy. *Diabetes.* (2016) 65:1099–108.

5. Katakami N, Omori K, Taya N, Arakawa S, Takahara M, Matsuoka T, et al. Plasma metabolites associated with arterial stiffness in patients with type 2 diabetes. *Cardiovasc Diabetol.* (2020) 19:75.

6. Hootman KC, Trezzi JP, Kraemer L, Burwell LS, Dong X, Guertin KA, et al. Erythritol is a pentose-phosphate pathway metabolite and associated with adiposity gain in young adults. *Proc Natl Acad Sci U.S.A.* (2017) 114:E4233–40. doi: 10.1073/pnas.1620079114

7. Schlicker L, Szebenyi DME, Ortiz SR, Heinz A, Hiller K, Field MS. Unexpected roles for ADH1 and SORD in catalyzing the final step of erythritol biosynthesis. *J Biol Chem.* (2019) 294:16095–108. doi: 10.1074/jbc.RA119.009049

8. Lee-Young RS, Hoffman NJ, Murphy KT, Henstridge DC, Samocha-Bonet D, Siebel AL, et al. Glucose-6-phosphate dehydrogenase contributes to the regulation of glucose uptake in skeletal muscle. *Mol Metab.* (2016) 5:1083–91. doi: 10.1016/j.molmet.2016.09.002

9. Ge T, Yang J, Zhou S, Wang Y, Li Y, Tong X. The role of the pentose phosphate pathway in diabetes and cancer. *Front Endocrinol.* (2020) 11:365. doi: 10.3389/fendo.2020.00365

10. Jin ES, Lee MH, Murphy RE, Malloy CR. Pentose phosphate pathway activity parallels lipogenesis but not antioxidant processes in rat liver. *Am J Physiol Endocrinol Metab.* (2018) 314:E543–51.

11. Kim J, Kim J, Bae JS. ROS homeostasis and metabolism: a critical liaison for cancer therapy. *Exp Mol Med.* (2016) 48:e269. doi: 10.1038/emm.2016.119

12. Ghanbari Movahed Z, Rastegari-Pouyani M, Mohammadi MH, Mansouri K. Cancer cells change their glucose metabolism to overcome increased ROS: one step from cancer cell to cancer stem cell? *Biomed Pharmacother.* (2019) 112:108690. doi: 10.1016/j.biopha.2019.108690

13. Zhao D, Badur MG, Luebeck J, Magaña JH, Birmingham A, Sasik R, et al. Combinatorial CRISPR-cas9 metabolic screens reveal critical redox control points dependent on the KEAP1-NRF2 regulatory axis. *Mol Cell.* (2018) 69:699–708.e7. doi: 10.1016/j.molcel.2018.01.017

14. Sapcariu SC, Kanashova T, Weindl D, Ghelfi J, Dittmar G, Hiller K. Simultaneous extraction of proteins and metabolites from cells in culture. *MethodsX.* (2014) 1:74–80.

15. Ortiz SR, Field MS. Chronic dietary erythritol exposure elevates plasma erythritol concentration in mice but does not cause weight gain or modify glucose homeostasis. *J Nutr.* (2021) 151:2114–24.

16. Bensadoun A, Weinstein D. Assay of proteins in the presence of interfering materials. *Anal Biochem.* (1976) 70:241–50.

17. Burg MB, Kador PF. Sorbitol, osmoregulation, and the complications of diabetes. *J Clin Invest.* (1988) 81:635–40.

18. Zhang DD, Hannink M. Distinct cysteine residues in keap1 are required for keap1-dependent ubiquitination of Nrf2 and for stabilization of Nrf2 by chemopreventive agents and oxidative stress. *Mol Cell Biol.* (2003) 23:8137–51. doi: 10.1128/MCB.23.22.8137-8151.2003

19. Ortiz SR, Field MS. Mammalian metabolism of erythritol: a predictive biomarker of metabolic dysfunction. *Curr Opin Clin Nutr Metab Care.* (2020) 23:296–301.

20. Weng Y, Fan X, Bai Y, Wang S, Huang H, Yang H, et al. SLC2A5 promotes lung adenocarcinoma cell growth and metastasis by enhancing fructose utilization. *Cell Death Discov.* (2018) 4:38. doi: 10.1038/s41420-018-0038-5

21. Chen WL, Jin X, Wang M, Liu D, Luo Q, Tian H, et al. GLUT5-mediated fructose utilization drives lung cancer growth by stimulating fatty acid synthesis and AMPK/mTORC1 signaling. *JCI Insight.* (2020) 5:e131596. doi: 10.1172/jci.insight.131596

22. Rzechonek DA, Dobrowolski A, Rymowicz W, Mirończuk AM. Recent advances in biological production of erythritol. *Crit Rev Biotechnol.* (2018) 38:620–33.

23. Bagnasco SM, Murphy HR, Bedford JJ, Burg MB. Osmoregulation by slow changes in aldose reductase and rapid changes in sorbitol flux. *Am J Physiol-Cell Physiol.* (1988) 254:C788–92. doi: 10.1152/ajpcell.1988.254.6.C788

24. Lenhart A, Chey WD. A systematic review of the effects of polyols on gastrointestinal health and irritable bowel syndrome. *Adv Nutr.* (2017) 8:587–96.

25. Ilouze M, Feinberg T, Shavit R, Peled N. Metabolic modification as a potential therapeutics approach in lung cancer. *Eur Respir J.* (2013) 42(Suppl. 57):4483.

26. Valdés A, Lucio-Cazaña FJ, Castro-Puyana M, García-Pastor C, Fiehn O, Marina ML. Comprehensive metabolomic study of the response of HK-2 cells to hyperglycemic hypoxic diabetic-like milieu. *Sci Rep.* (2021) 11:5058. doi: 10.1038/s41598-021-84590-2

27. Eggleston LV, Krebs HA. Regulation of the pentose phosphate cycle. *Biochem J.* (1974) 138:425–35.

28. Cossu V, Bonanomi M, Baucknehtt M, Ravera S, Righi N, Miceli A, et al. Two high-rate pentose-phosphate pathways in cancer cells. *Sci Rep.* (2020) 10:22111. doi: 10.1038/s41598-020-79185-2

29. Aurora AB, Khivansara V, Leach A, Gill JG, Martin-Sandoval M, Yang C, et al. Loss of glucose 6-phosphate dehydrogenase function increases oxidative stress and glutaminolysis in metastasizing melanoma cells. *Proc Natl Acad Sci.* (2022) 119:e2120617119. doi: 10.1073/pnas.2120617119

30. Valayannopoulos V, Verhoeven NM, Mention K, Salomons GS, Sommelet D, Gonzales M, et al. Transaldolase deficiency: a new cause of hydrops fetalis and neonatal multi-organ disease. *J Pediatr.* (2006) 149:713–7. doi: 10.1016/j.jpeds.2006.08.016

31. Verhoeven NM, Huck JHJ, Roos B, Struys EA, Salomons GS, Douwes AC, et al. Transaldolase deficiency: liver cirrhosis associated with a new inborn error in the pentose phosphate pathway. *Am J Hum Genet.* (2001) 68:1086–92. doi: 10.1086/320108

32. Mitsuishi Y, Taguchi K, Kawatani Y, Shibata T, Nukiwa T, Aburatani H, et al. Nrf2 redirects glucose and glutamine into anabolic pathways in metabolic reprogramming. *Cancer Cell.* (2012) 22:66–79. doi: 10.1016/j.ccr.2012.05.016

33. Tang YC, Hsiao JR, Jiang SS, Chang JY, Chu PY, Liu KJ, et al. c-MYC-directed NRF2 drives malignant progression of head and neck cancer via glucose-6-phosphate dehydrogenase and transketolase activation. *Theranostics.* (2021) 11:5232–47. doi: 10.7150/thno.53417